Microfluidic Gate

Utilization of Self-Assembling, Free-Flowing Superstructures of Superparamagnetic Beads for Enhanced Mixing and Colloidal Separation

Bernhard Eickenberg, Frank Wittbracht, Andreas Hütten
Department of Physics, Thin Films and Physics of Nanostructures
University of Bielefeld
Bielefeld, Germany
e-mail: beickenb@physik.uni-bielefeld.de

Alexander Weddemann
Department of Electrical Engineering and Computer Science
Massachusetts Institute of Technology
Cambridge, USA

***Abstract*— Due to dipolar interactions, superparamagnetic beads self-assemble into one- and two-dimensional superstructures under the influence of a homogeneous magnetic field. When the magnetic field is adiabatically rotated in-plane, the superstructures follow the rotation. We developed a microfluidic device in which the rotation of these agglomerates is used to simultaneously enhance mixing and allow for colloidal separation. The device shows high separation efficiencies. When taking the mass separation rate into account, the optimal working regime of the device lies around 120 µm/s, where it yields 80% of the total amount of beads.**

Keywords- microfluidics; superparamagnetic beads; dipolar coupling; reconfigurable matter; rotating magnetic fields.

I. INTRODUCTION

Due to promising applications in biomedical analysis, superparamagnetic beads have been thoroughly studied during the last decades [1-3]. Their surface functionalization allows the specific binding of biomolecules like DNA or proteins[4,5] whereas the permanent magnetic moment of the particles makes it possible to manipulate their movement in microfluidic channels through external magnetic fields [6-8] or detect them with magnetoresistive sensors [9-11]. This makes them applicable as carriers or markers for biomedical diagnostics in lab-on-a-chip systems.

Another promising application is the utilization of the beads as reconfigurable matter [12]: Under the influence of a homogeneous magnetic field, the magnetic moment vectors align parallel to the external field. This alignment leads to an increase in the effective magnetization and thus results in a higher magnetic stray field. Since the stray field is inhomogeneous, adjacent particles attract each other and form one- (chains) or two-dimensional (clusters) superstructures [13-15]. Once the magnetic field is removed, the superstructures disassemble on a time scale of several seconds.

Just like the particles, superstructures can be manipulated with external magnetic fields as their orientation follows the direction of the field. Therefore, adiabatic rotation of the field leads to rotation of the agglomerates [16] which can be utilized to enhance mixing in microfluidic devices, as demonstrated by Lee et al. [17] and Sawetzki et al. [18]. They used microfluidic chambers and optical tweezers to confine magnetic assemblies in microfluidic compartments and utilize them as active micromixers.

In this work, the formation and rotation of superstructures composed of superparamagnetic beads is employed to design a combined microfluidic system which enables enhanced fluid mixing and colloidal separation. Figure 1 shows the overview of the separation mechanism of the device: Superparamagnetic beads form one- and two-dimensional rotating superstructures under the influence of an external homogeneous magnetic field. At the separation junction (two diverging channels separated by a barrier) the rotation of the agglomerates leads to a transversal movement due to interactions of the superstructures with the barrier. The direction of this movement depends on the orientation of the rotation (clockwise or counter-clockwise). Thus, the flow of agglomerates can be limited to either one of the two diverging channels, depending on the parameters of the external field. If no magnetic field is applied, the individual particles are distributed statistically over both channels.

At the T-junction (depicted in Figure 2), the rotation of the superstructures leads to a perturbation of the boundary layer between the two parallel, laminar flows. A convective fluid flux from the upper layer into the lower layer and *vice versa* is created and leads to enhanced mixing. Without the rotation, thermal diffusion would be the only driving force for mixing. Unlike the other magnetic mixing devices mentioned above, this device utilizes free-flowing components that can be assembled in real-time.

 ISBN: 978-1-61208-151-9

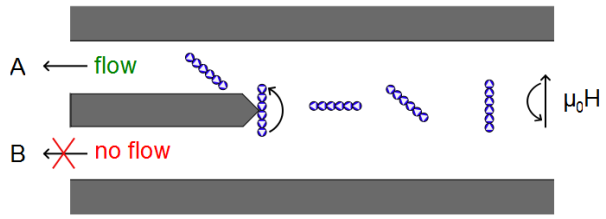

Figure 1. Operation principle of the microfluidic gate: The rotation of the superstructures leads to a transversal movement of the agglomerates at the separation junction. The direction of the movement depends on the orientation of the rotation of the magnetic field. Thus, the particle flow can be restricted to one channel.

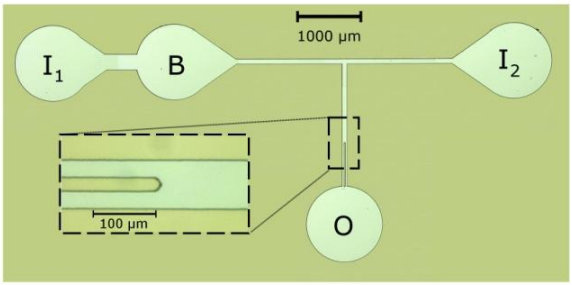

Figure 2. Microscopy image of the SU8-3025 casting mold with the inlet reservoirs I_1 and I_2, the outlet reservoir O and the bead reservoir B. The small image shows a magnification of the separation junction.

In this paper, we describe the experimental realization of the proposed microfluidic device. In the results section, both the performance of the colloidal separation and the mixing enhancement are evaluated.

II. EXPERIMENTAL

The microfluidic structure was created by soft-lithography techniques [19]. Figure 2 shows a microscopy image of the SU8-3025 casting mold. The actual channel system was made from PDMS that was sealed with a silica wafer by plasma oxidation of the surfaces.

The structure consists of two inlet reservoirs I_1 and I_2 that are connected to a T-junction *via* channels of 77 µm width. A bead reservoir B is used to introduce beads into the system. The main channel connecting the T-intersection with the outlet reservoir O has a width of 79 µm and is split into two channels of 28 µm width by a 23 µm wide barrier. Liquid flow is induced by hydrostatic pressure.

Dynabeads MyOne^{TM} beads with a mean diameter of 1.05 µm at a standard deviation of 1.9% were chosen for the experiments [20]. The bead surface is covered with carboxylic acid ligands. The mass saturation magnetization of the MyOne^{TM} beads is 23.5 Am^2/kg. For the experiments, a stock solution of 10 mg/mL was diluted with deionized water to a final concentration of 120 µg/mL. Reservoir B was then filled with this solution, whereas I_2 was filled with a 65 mM solution of flavin adenine dinucleotide (FAD) to allow for optical evaluation of the mixing behavior. The ratio of the flow from I_1 and I_2 to O, respectively, was adjusted *via* the water level in I_1.

A modified RCT basic (IKA) magnetic stirrer with a maximum in-plane field strength of 690 Oe was placed beneath the microfluidic chip to provide the rotating magnetic field. The field strength leads to a degree of saturation of 73% in the MyOne^{TM} beads. A rotation frequency of 50 rpm was chosen for the whole experiment.

For evaluation, the amount of chains (transversal width of one or two beads) and clusters (transversal width of three or more beads) passing through channel A and B was counted separately. Superstructures fracturing at the barrier were counted as flowing through both channels. The ratio of beads flowing through channel A and B was obtained through the ratio of the area of the superstructures. Flow velocities were evaluated by tracking of superstructures in the channel.

III. RESULTS AND DISCUSSION

The influence of the rotating bead superstructures on the boundary layer between the water and the FAD solution can be seen in the optical microscopy images displayed in Figure 3. The interface between the two flows is highlighted in red. Due to hydrodynamic interactions with the surrounding fluid, the rotating agglomerates create a transversal convective flow that enhances the mixing of the two parallel streams. This way, they are acting as free-flowing magnetic microstirrers that can be easily assembled and disassembled on demand in real-time.

At the separation junction, the interaction of the bead agglomerates with the barrier leads to a colloidal separation as described in Figure 1. Depending on the chosen direction

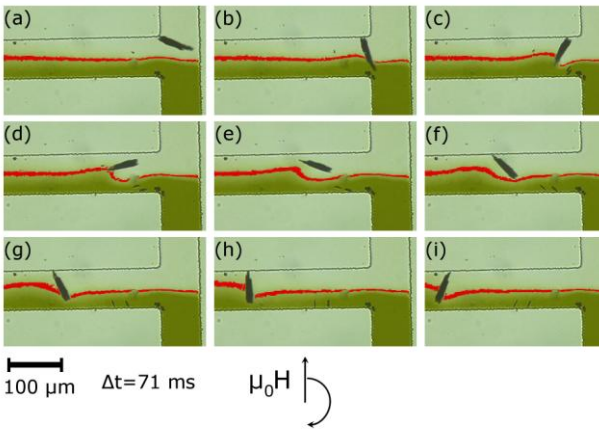

Figure 3. Microscopy images of the fluid interface at the T-junction. The rotation of the superstructures causes a convective flux orthogonal to the flow direction, thus enhancing mixing. The interface between the two liquids is highlighted in red. For better perceptibility, the contrast of the yellow FAD was increased.

 ISBN: 978-1-61208-151-9

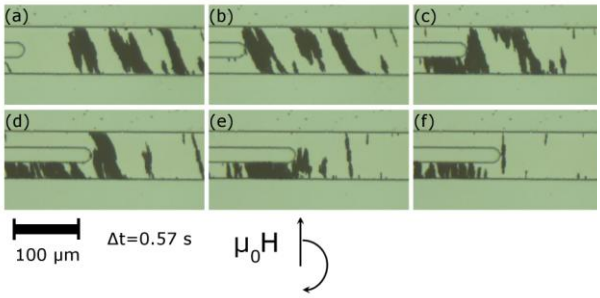

Figure 5. Optical microscopy images showing the separation of cluster agglomerates. Even at high local bead densities, the separation is efficient and no clogging of the channels is observed.

of the magnetic field rotation, the particle flow can be restricted to the upper or lower channel. As can be seen from the optical microscopy images in Figure 4, even high bead densities can be successfully guided. Figure 5 shows a series of optical microscopy images of the separation process. Through the effect of the clockwise rotation, the one-(5-a) and two-(5-b) dimensional bead agglomerates are guided into the lower channel. Only at higher flow velocities above 100 µm/s, breakage of chains (5-c) or even clusters (5-d) occurs at the separation barrier due to high

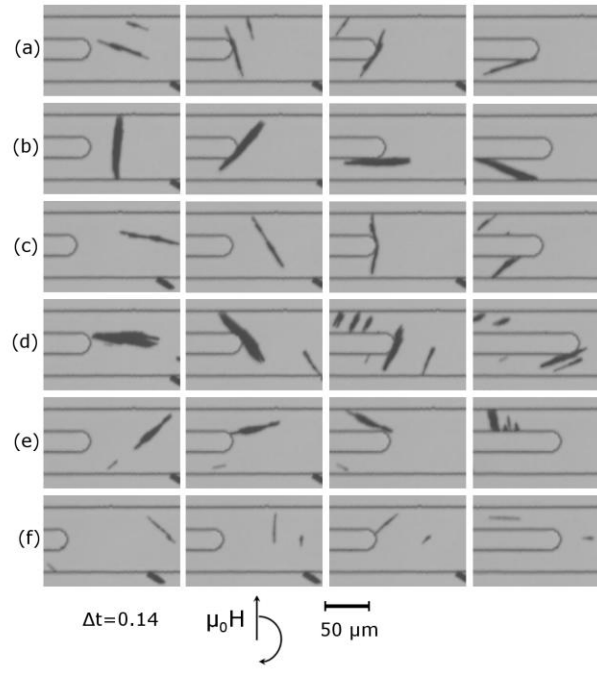

Figure 4. Even at flow velocities of 274 µm/s, chains (a) and clusters (b) can be guided into the lower channel by clockwise rotation of the magnetic field. At these flow velocities, however, chains (c) and clusters (d) may fracture at the separation barrier due to shear induced stresses. Additionally, due to the high velocity, some superstructures pass the separation junction without interacting with the barrier (e). At all flow velocities, occasional fragments (f) with lateral dimensions smaller than the channel diameter pass the junction without being guided.

shear induced stresses, thus reducing the separation efficiency. Additionally, fragments with lateral dimensions smaller than the width of the diverging channels cannot be guided successfully, since they often passed the separation junction without interacting with the barrier (5-f). However, they do not significantly lower the separation efficiency as the amount of beads per fragment is insignificantly low. In contrast to breakage of clusters, the presence of fragments is visible at all flow velocities. Adjustment of the bead concentration and the parameters for the chain formation process might reduce the amount of fragments, though.

The evaluation of the separation efficiency was performed for clockwise rotation. Figure 6 shows the fraction of chains, clusters and total amount of beads that was successfully guided into the lower channel B. At low mean flow velocities (42 and 63 µm/s) more than 90% of the superstructures are successfully separated. The low percentage of particles flowing through channel A can be attributed to the fragments mentioned above which do not interact with the separation barrier. When the flow velocity is increased to 120 µm/s, the overall separation yield slightly decreases to 89% due to the increased probability of chain breakage: Only 71% of the chains are guided into the lower channel, whereas most of the clusters (84%) remain stable and resist the fragmentation by shear induced stress. At high flow velocities of 274 µm/s, cluster breakage becomes more common and reduces the ratio of guided clusters to 61%. At these high velocities, several clusters pass the separation junction without performing a 180° rotation, so that they reach channel A without interacting with the barrier (5-e), thus decreasing the separation yield. This effect could be counteracted by increasing the rotation frequency of the magnetic field, though a higher rotation speed might increase the probability of cluster breakage. Still, 63% of the total amount of beads are successfully guided into the lower channel, showing that a significant separation can still be achieved at these velocities.

To analyze the efficiency of the design, we define the separation efficiency ε as follows:

$$\varepsilon = (x - 0.5)/0.5 \qquad (1)$$

with x as the fraction of separated beads. Thus, ε takes into account that without the application of an external field, 50% of the beads would be guided into each of the two diverging channels. Figure 6 shows the values of ε depending on the flow velocity. For velocities of up to 120 µm/s, high efficiencies between 0.92 and 0.77 are obtained. Only at higher flow velocities of 274 µm/s the efficiency drops to 0.26. However, higher flow velocities mean that a larger volume and therefore a higher amount of beads is transported and guided per time. We therefore introduce the mass separation rate ξ as

$$\xi = \Gamma \cdot c_{Bead} \cdot \varepsilon \qquad (2)$$

 ISBN: 978-1-61208-151-9

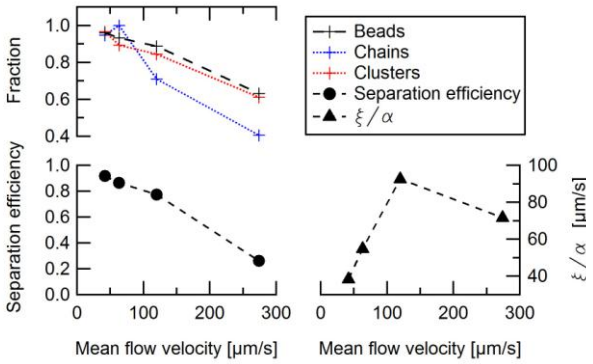

Figure 6. Evaluation of the separation performance. (a) The fraction of the total amount of beads and of chain/cluster superstructures guided into channel B. (b) Development of the separation efficiency ε with the mean flow velocity. (c) Development of the quantity ξ/α with the mean flow velocity. The optimal working regime for the device lies around 120 µm/s.

with c_{bead} as the bead concentration and Γ as the volume flow rate which is given by

$$\Gamma = |\mathbf{u}| \cdot A \quad (3)$$

with $|\mathbf{u}|$ as the flow rate and A as a geometry parameter. Since c_{bead} and A do not depend on the flow velocity but only on experimental conditions which were not changed during the presented experiments, we introduce the experimental parameter α:

$$\alpha = c_{Bead} \cdot A \quad (4)$$

Figure 6 shows the progression of the quantity ξ/α, which takes all flow velocity dependent effects into account, with the flow velocity. The plot shows an increase of the device efficiency from 38 µm/s to 93 µm/s when increasing the flow velocity from 42 µm/s to 120 µm/s. A further increase of the velocity decreases the efficiency to a value of 72 µm/s. Thus we can deduce that the optimal working regime for the device lies around 120 µm/s for an operation frequency of 50 rpm.

IV. CONCLUSION

The proposed microfluidic design offers simultaneous enhancement of fluid mixing and highly efficient colloidal separation through the use of self-assembling, free-flowing superstructures that can be built and disassembled on a time scale of several seconds. The structure can be realized by application of an external homogeneous time-dependant field without the need for micro-structured components. The optimal working regime for the device lies around a flow velocity of 120 µm/s for rotation frequencies of 50 rpm.

In future work, the presented design will be used to separate biomolecules from a biological sample matrix and localize them on the bead surface, allowing for detection without background interference by the matrix components.

ACKNOWLEDGMENT

The authors thank the FOR 945 for financial support in the framework of project 3. Alexander Weddemann gratefully acknowledges the Alexander-von-Humboldt-Foundation for financial support.

REFERENCES

[1] N. Pamme, “Magnetism and microfluidics”, Lab Chip, vol. 6(1), 2006, pp. 24-38.

[2] E. Verpoorte, “Beads and chips: new recipes for analysis”, Lab Chip, vol. 3(4), 2003, pp. 60N-68N.

[3] M. A. M Gijs, “Magnetic bead handling on-chip: new opportunities for analytical applications”,Microfluid. Nanofluid., vol. 1(1), 2004, pp. 22-40.

[4] Z. H. Fan, S. Mangru, R. Granzow, P. Heaney, W. Ho, Q. Dong, and R. Kumar, “Dynamic DNA hybridization on a chip using paramagnetic beads”, Anal. Chem., vol. 71, 1999, pp. 4851-4859.

[5] F. G. Pérez and M. Mascini, “Immunomagnetic separation with mediated flow injection analysis amperometric detection of viable Escherichia coli O157”, Anal. Chem., vol. 70, 1998, pp. 2380-2386.

[6] L. E. Johansson, K. Gunnarsson, S. Bijelovic, K. Eriksson, A. Surpi, E. Göthelid, P. Svedlindh, and S. Oscarsson, “A magnetic microchip for controlled transport of attomole levels of proteins”, Lab Chip, vol. 10, 2010, pp. 654-661.

[7] T. Deng, G. M. Whitesides, M. Radhakrishnan, G. Zabow, and M. Prentiss, “Manipulation of magnetic microbeads in suspension using micromagnetic systems fabricated with soft lithography”, Appl. Phys. Lett., vol. 78 (12), 2001, pp. 1775-1777.

[8] M. Panhorst, P. B. Kamp, G. Reiss, and H. Brückl, “Sensitive bondforce measurements of ligand-receptor pairs with magnetic beads, Biosens. Bioelectron., vol. 20(8), 2005, pp. 1685-1689.

[9] D. L. Graham, H. A. Ferreira, and P. P. Freitas, “Magnetoresistive-based biosensors and biochips, Trends in Biotechnology, vol. 22(9), 2004, pp. 455-462.

[10] V. C. Martins, J. Germano. F. A. Cardoso. J. Loureiro, S. Cardoso, L. Sousa, M. Piedade, L. P. Fonseca, and P. P. Freitas, “Challenges and trends in the development of a magnetoresistive biochip portable platform”, J. Magn. Magn. Mater., vol. 322, 2010, pp. 1655-1663.

[11] C. Albon, A. Weddemann, A. Auge, K. Rott, and A. Hütten, „Tunneling magnetoresistance sensors for high resolutive particle detection“, Appl. Phys. Lett., vol. 95(2), 2009, 023101.

[12] P. S. Doyle, J. Bibette, A. Bancaud, and J.-L. Viovy, “Self-assembled magnetic matrices for DNA separation chips”, Science, vol. 295(22), 2002, p. 2237.

[13] S. Melle, O. G. Calderon, M. A. Rubio, and G. G. Fuller, “Microstructure evolution in magnetorheological suspensions governed by Mason number”, Phys. Rev. E, vol. 68, 2003, 041503.

[14] A. Weddemann, F. Wittbracht, B. Eickenberg, and A. Hütten, “Magnetic field induced assembly of highly ordered two-dimensional particle arrays”, Langmuir, vol. 26, 2010, pp. 19225-19229.

[15] A. Weddemann, F. Wittbracht, A. Auge, and A. Hütten, “Particle flow control by induced dipolar interaction of superparamagnetic microbeads”, Microfluid. Nanofluid., vol. 10(2), 2011, pp. 459-463.

[16] A. K. Vuppu, A. A. Garcia, and M. A. Hayes, “Video microscopy of dynamically aggregated paramagnetic particle chains in an applied rotating magnetic field, Langmuir, vol. 19, 2003, pp. 8646-8653.

[17] S. H. Lee, D. van Noort, J. Y. Lee, B.-T. Zhang, and T. H. Park, “Effective mixing in a microfluidic chip using magnetic particles”, Lab Chip, vol. 9, 2009, pp. 479-482.

[18] T. Sawetzki, S. Rahmouni, C. Bechinger, and D. W. M. Marr, „In situ assembly of linked geometrically coupled microdevices“, PNAS, vol. 105, 2008, pp. 20141-20145.

[19] J. Friend and L. Yeo, “Fabrication of microfluidic devices using polydimethylsiloxane”, Biomicrofluidics, vol. 4, 2010, 026502.

 ISBN: 978-1-61208-151-9

[20] G. Fonnum, C. Johannson, A. Molteberg, S. Mørup, and E. Aksnes, “Characterisation of Dynabeads ® by magnetization measurements and mossbauer spectroscopy”, J. Magn. Magn. Mat., vol. 293, 2005, pp. 41-47.

 ISBN: 978-1-61208-151-9